The Influence of Multilive Feed Processing and Fibre Length on the Stiffness and Strength of Injection Moulded 50% w/w Glass/Nylon 6,6 Composites

R.S. Bailey, G. v. Bradsky, S.I. Naqui, I.M. Robinson* and J.M. Robinson

ICI Wilton Research Centre, Wilton, Cleveland TS90 8JE, U.K.

ABSTRACT

'he influence of fibre aspect ratio on multilive feed ;lass fibre/nylon 6,6 composites has been studied using wo model materials based on extrusion and pultrusion ompounding. Characterisation of the microstructure of hese compounds revealed that the fibre orientation listribution and volume fraction were similar between he compounds, but the fibre length distributions were bund to be different, with the compound produced by ultrusion compounding having the larger mean fibre spect ratio. The mechanical performance of the two ompounds was evaluated in terms of stiffness and trength across a wide range of service conditions using oth tensile dilatometry and creep deformation. Under ll test conditions, an improved level of mechanical erformance was seen for compounds with improved nean fibre aspect ratio. Modelling these materials in erms of stiffness and strength also revealed that mproved performance is expected with an improved ibre aspect ratio.

KEYWORDS

:tiffness, strength, microstructure, discontinuous fibre :omposite, fibre aspect ratio

1. INTRODUCTION

The general influence of processing on the properties of njection moulded components is perhaps better understood for the more traditional fibre reinforced thermoplastics, based on extrusion compounding, than the newer ones, based on both materials and processing improvements /1/. Multiple-live-feed injection moulding /2/ exemplifies a processing innovation, whilst injection moulded feedstock based on pultruded granules, rather than extrusion compounded granules /3/, illustrates a material innovation. Multiple-live feed injection moulding is known to influence the microstructure of such materials, with an improvement in fibre orientation at the expense of increased fibre degradation. Pultruded material provides moulded components with longer fibre reinforcement compared with the extrusion compounded equivalent and this is known to influence both processing and microstructure and in turn to benefit material properties /4,5/.

Fibre reinforced thermoplastic compounds behave in a viscoelastic manner and are also anisotropic. Consequently such behaviour must be incorporated into a description of their material properties.

In a general sense the stiffness of such materials can be described as follows:

$$E_c = E(E_f, V_f, FLD, FOD, \gamma, E_m(t, T, \epsilon, C), \theta, etc) \quad (1)$$

where

E_c = Modulus for compound
V_f is the fibre volume fraction
FLD is the fibre length distribution
FOD is the fibre orientation distribution
γ is some function of interfacial adhesion between fibre and matrix

* Present address:
Courtaulds Research and Technology, PO Box 111, Lockhurst Lane, Coventry CV6 5RS, U.K.

E_m = modulus for the matrix material (dependent upon the next four variables)
t is the time under load
T is the temperature
ε is the strain level
C is the conditioning
Θ is the angle between the principal stress and mould fill direction

The first four variables are determined by the constituent fibres and the resultant microstructure in the moulding. The adhesion is a property of both the fibre and matrix. The influence of time, temperature and strain are viscoelastic effects on the matrix and the conditioning is an environmentally controlled variable which may alter the matrix and the degree of adhesion. The direction of applied stress may be altered in selected test specimens and the mode of loading.

Each of these variables will influence the resultant modulus for the compound, although it is not clear from the general form of equation (1) which of the variables are more important than others. The influence of some of these parameters has been examined in many publications. In particular, the influence of the matrix viscoelastic response due to time, temperature and strain is well known. More is becoming apparent on the influence of anisotropy whilst processing would benefit from further research.

With these developments in mind, the general theme of this paper is to examine two categories of fibre reinforced thermoplastic compounds, based on extrusion compounding and pultrusion granulation with a common fibre and thermoplastic matrix (glass fibre and nylon 6,6) at constant volume fraction under the influence of multiple-live-feed moulding conditions in a common mould. Such a strategy encompasses a common material and mould format. The study has been restricted to examining in detail the stiffness and strength in tension, and the stiffness in flexure and torsion as a function of key matrix variables such as temperature, time under load, etc. This should easily identify the distinct advantage in mechanical performance that pultrusion based compounds possess with increased fibre length over their extrusion compounded based rival, in a controlled microstructure achieved through the use of multiple-live feed process technology across a range of likely service conditions. Comparison of the resultant engineering data to existing data for these materials based on standard injection moulding processing should enable a designer to consider the multi-live feed data to be of use for general design.

The work is presented in three parts:

(i) The preparation of the injection moulded plaques and their morphological characterisation in terms of fibre orientation distribution, through thickness heterogeneity, fibre length analysis and fibre content. This is dealt with in sections 2 and 3.

(ii) Mechanical characterisation of the mouldings in terms of short term stiffness as determined from tensile dilatometry, and under creep loading in tension, flexure and torsion. The mechanical properties examined have been determined at 23°C under dry conditions and after exposure to moisture conditioning. In addition a range of higher service conditions in terms of temperature, time and conditioning have been explored. Tensile creep tests will be reported, performed at a range of elevated temperatures up to a limit of 120°C. The mechanical characterisation is reported in section 4.

(iii) Modelling the short term stiffness and strength of these materials and seeing what influence the effect of fibre length and temperature has on the predicted stiffness and strength. This is described in section 5.

In all aspects of the work there is an intention to establish a property-structure link in the evaluations with the specific aim of understanding performance of the materials.

2. SAMPLE PREPARATION

The two injection moulding materials were both based on 50% w/w (30% by volume) glass fibre reinforced nylon 6,6. The short fibre reinforced compound was prepared by commercial extrusion compounding whilst the long fibre reinforced material was prepared by pultrusion from which granules for injection moulding were cut. The length of these granules was 10 mm and this equalled the length of continuous glass present in the injection moulding feedstock. (This was subsequently reduced by the moulding process.) The glass fibre diameters differed between the materials; the short fibre reinforced compound used a diameter of 10µm whereas the long fibre reinforced compound used a fibre diameter of 17µm. The compounds were ICI Materials products and commercial versions are available under the trade names of Maranyl A690 and Verton RF700-10, respectively. For the study presented here the compounds are abbreviated using the nomenclature shown below:

Compound	Moulding Process
	Multiple-Live Feed Moulding
Verton RF700-10	Long GL/PA MLF
Maranyl A690	Short GL/PA MLF

The mould used was 180 mm x 60 mm, with gates centred about each end and mouldings were produced at 3 mm thickness. Figure (1) shows a schematic representation of the mould. The mouldings were produced at Brunel University, using the multiple live feed injection moulding process as described by Allan and Bevis /1/. The moulding conditions were optimised for both materials in order that the moulding cycle should be as similar for each as possible. Specimens appropriate for the test geometry were machined from these plaques in order to conduct a range of stiffness and strength tests. The specimens were all such that the applied stress aligned with the mould fill direction. Consequently all the specimens tested in this study can be described as having 0° orientation.

3. MORPHOLOGICAL CHARACTERISATION

The samples produced from the two distinct materials should show clear differences in the fibre length distribution whilst retaining similar fibre orientation distributions and volume fractions and to this end a number of tests have been performed to resolve these key microstructural parameters. The fibre orientation distribution was examined by image analysis, the fibre length distribution in each type of compound by image analysis/optical microscopy and the fibre volume fractions a standard method involving weight fractional analysis.

3.1. Fibre Orientation Distribution (FOD) by Image Analysis

The Fibre Orientation Distribution (FOD) for each type of sample state was analysed using a Kontrol AT386 hosted Image Analyser /7/. The software measures the local spatial orientations of short and long fibre reinforced thermoplastics. Since an exact prediction of the FOD from the flow conditions of the melt is not at present possible, a concept has been developed for measuring this parameter in moulded parts. This has been comprehensively reviewed in reference /8/. The moulded part is sectioned and polished and may be imaged either by SEM or by optical microscopy with the use of a scanning table. For this work, sections from the centre of the specimens were polished in the three planes: XY, XZ and YZ as indicated in Figure 1. It should be noted that the polishing process is critical to the success of the FOD measurements as fibre definition is an essential requirement in the subsequent image analysis procedure.

After goal coating, the samples were examined by SEM (Hitachi 5520) using a high KV to generate optimum contrast in the images for subsequent automatic image analysis. A more detailed report on the conditions necessary for image analysis is given in reference /7/. SEM micrographs were taken parallel to the edge of the sections to ensure that the axes directions remained constant. A series of micrographs were taken across the thickness of the section to the central line. A field of view was chosen to be approximately 500µm. This allowed high enough resolution to accurately identify fibres for image analysis, whilst still remaining within the practical limits of the technique in terms of time and effort. The field of view is further subdivided into 2 frames which consequently provide FOD data every 250µm in depth.

Once the grey tone image has been processed and thresholded into a binary format, image analysis algorithms were applied to the features of interest (namely the fibre cross sections).

The method of measuring the spatial FOD is

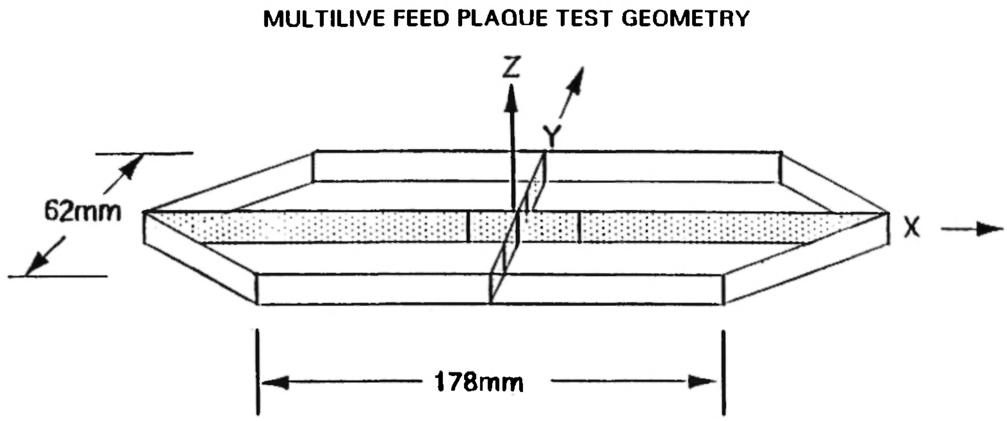

Fig. 1: Multilive feed plaque test geometry

founded on the fact that cross sections of fibres with infinite lengths always have elliptical shapes. The ratio of the two main axes of the ellipse depends on the angle of inclination to the section plane (out of plane angle, ß). The orientation of the fibre in the sectioning plane is equal to the orientation of the longer major axis of the cross section (in plane angle, α) /8/ to within an accuracy of approximately ± 6° for fibres perfectly aligned.

Using angles α, ß each fibre can be described as a 3-D orientation vector:

$$P = \begin{pmatrix} P_x \\ P_y \\ P_z \end{pmatrix} = \begin{pmatrix} \cos\beta\cos\alpha \\ \cos\beta\sin\alpha \\ \sin\beta \end{pmatrix} \quad (2)$$

The vector components are normalised by squaring and average orientation factors can be calculated as the mean values of the squared components, the values of which lie between 0.0 and 1.0 which corresponds from poor to excellent fibre alignment. The average orientation factors are quantified for the field of view in the x, y and z directions.

The automatic image analyses were performed on micrographs taken through the thickness of the plaque specimens. The XZ plane was chosen to generate all profile data; the reasons for this are discussed in /7/. The data contained in Table 1 gives the profiles of orientation factors in the x, y and z directions taken in the XZ plane from the surface of the mouldings to the centre of the plaque mouldings. The data contained in Table 1 has been converted into α (in plane) and ß (out of plane) angles and are reported in Table 2.

The data contained in Tables 1 and 2 indicate that the fibre orientation distributions for Long and Short GL/PA MLF mouldings are similar, although the Short GL/PA MLF moulding shows slightly less alignment.

Processing using the MLF method appeared to influence significantly the spatial FOD and the microstructure, particularly in the core compared to that seen in conventionally moulded compounds /9-11/.

The higher alignment in the core is due to the pulsed flow giving rise to a more oriented core owing to the formation of an aligned skin during each pulse. The resultant structure differs from the conventionally moulded specimen predominantly in the core and transitional regions. Once the mould is full, the skin arising from the mould filling will be similar. The MLF method also holds a higher alignment of fibres throughout the specimen thickness, with the size of the core much reduced. A further point of interest is the smooth transition of the FOD shown in Figure (2), which is likely to result from the actual oscillating pulses.

A final comment relates to the out of plane behaviour of the materials. In all samples it is evident that the out of plane orientation factor F(z) increases with depth into the section, indicating greater freedom of movement experienced by the fibres. However the Long GL/PA MLF specimens do show less freedom and out of plane orientation than the Short GL/PA MLF compounds. This correlates with the fact that spatial hindrance is alleged to be a dominant factor in mould filling owing to two effects:

a) The shear experienced by the melt is higher through the mould thickness;
b) The fibres are restricted by their length in out of plane mobility, particularly for Long GL/PA compounds.

Overall the FOD between the two compounds could be seen to be similar, so that this aspect of microstructure is common between the Long and Short GL/PA MLF mouldings.

3.2. Fibre Length Distributions

Fibre lengths were measured by image analysis/optical microscopy method (Seescan Satellite/Olympus Stereo Microscope) from fibres released from the polymer matrix by pyrolysis. The results are given below in Table 4. The fibres remaining from pyrolysis in this type of material retain their structure as imposed by the injection moulding process. As a result, the skin and core can be identified as distinct layers and fibres may be extracted from each region with ease. This serves to increase the relative accuracy of the fibre length results and to provide more morphological information regarding the degree of fibre attrition resulting from the shear history, and enables the local fibre length data to be used directly in modelling the microstructure.

Table 1

Orientation factors in the X, Y and Z directions, taken in the XZ plane for both the Long GL/PA and Short GL/PA MLF compounds

Orientation Factors						
	Long GL/PA MLF			Short GL/PA MLF		
Depth from surface um	X	Y	Z	X	Y	Z
0 - 250	.713	.239	.043	.731	.223	.046
250 - 500	.825	.130	.040	.737	.206	.057
500 - 750	.709	.230	.070	.624	.309	.067
750 - 1000	.760	.195	.040	.417	.446	.137
1000 - 1250	.656	.284	.059	.618	.315	.068
1250 - 1500	.551	.335	.072	.434	.473	.093

Table 2

Orientation angles in the α (in plane) and ß (out of plane) directions, given in degrees, for both the Long GL/PA and Short GL/PA MLF compounds

Orientation Angles				
	Long GL/PA MLF		Short GL/PA MLF	
Depth from surface um	α	β	α	β
0 - 250	29.9	11.9	28.9	12.4
250 - 500	21.6	11.5	27.9	13.8
500 - 750	29.8	15.3	35.1	15.0
750 - 1000	26.8	11.5	46.0	21.7
1000 - 1250	33.3	14.1	35.6	15.1
1250 - 1500	36.9	15.6	46.2	17.7

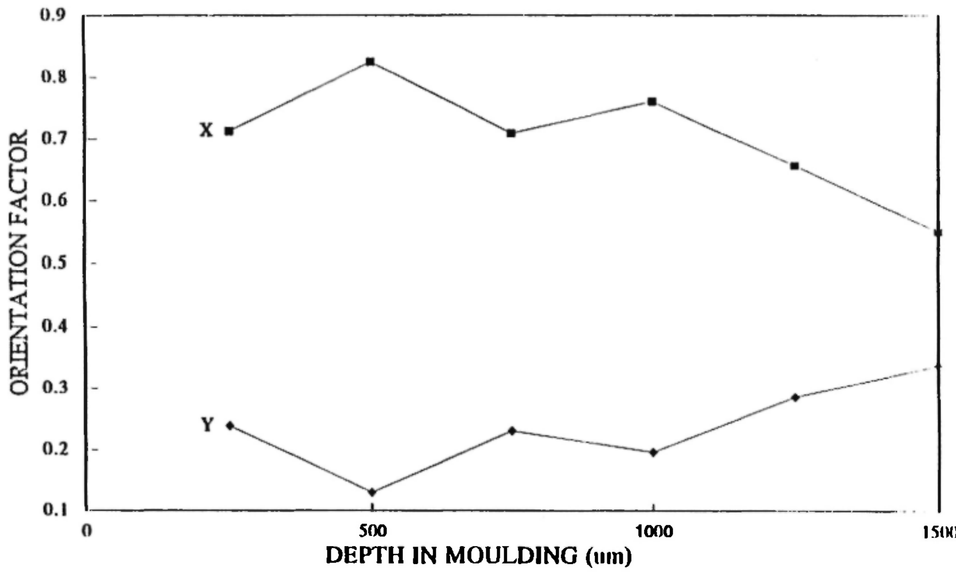

Fig. 2 Profile of orientation factors for LF GL/PA MLF moulding

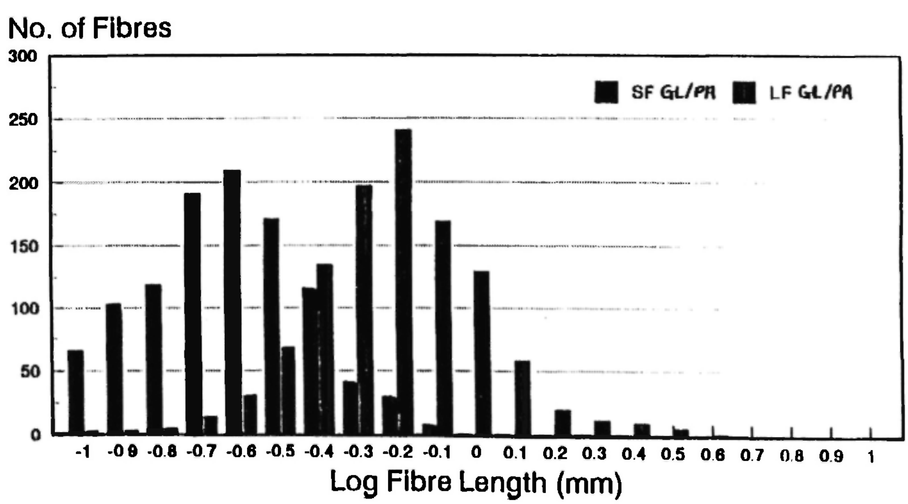

Fig. 3 Fibre length distributions for LF GL/PA and SF GL/PA Multifeed processed 50% w/w glass

The fibre length distributions are similar in the skin and core regions for the samples based on the same processing route. Typical fibre length distributions from the skin region for these types of materials are shown in Figure (3). The numbers given in parenthesis are two standard deviations from the mean value and represent the limits of the distribution such that 95% of all fibres are found within the two limits. The results indicate that the mean length for the Long GL/PA MLF compound is approximately a factor of 2.5 times longer than that achieved by the Short GL/PA MLF compound. It is also worth noting that less than 2.5% of fibres for the Long GL/PA MLF compound have lengths that are equal to or less than the mean fibre

Table 3

Mean fibre length determined from an average of 1000 fibres in the skin and core region of the Long and Short GL/PA MLF mouldings. The mean was calculated from the histogram of log fibre length. The numbers given in parenthesis are two standard deviations from the mean value and represent the limits of the distribution such that 95% of all fibres are found within the two limits.

Sample	Skin Mean Fibre Length (mm)	Core Mean Fibre Length (mm)
Long GL/PA MLF	0.58 (0.18, 1.89)	0.55 (0.20, 1.51)
Short GL/PA MLF	0.21 (0.08, 0.53)	0.21 (0.08, 0.53)

Table 4

Mean critical aspect ratios (mean fibre length/diameter) for all samples studied, determined from the data in Table 3.

Sample	Mean Critical Aspect Ratio
Long GL/PA MLF	34
Short GL/PA MLF	21

length for the Short GL/PA MLF moulding as determined from the standard deviations of the two distributions.

Clearly the Long GL/PA MLF compounds have a longer fibre length distribution than the Short GL/PA MLF compound. It is also worth stressing that the multiple live-feed process has reduced the mean fibre length in the long fibre compound compared to that normally seen in conventionally moulded components, an effect reported elsewhere /10-12/. The reduction in fibre length has effectively reduced the number of very long fibres seen in the fibre length distribution and effectively made the distribution more gaussian, as can be seen in Figure (3). A reduction in mean fibre length has also occurred for the short fibre compound, though not to the same extent as that found for the long fibre compound.

The mean critical aspect ratios (mean fibre length/diameter) for the materials are given below.

The effect these values have in relation to the stiffness in discontinuous fibre composites will be explained in section 5.

3.3. Fibre Volume Fractions

Volume fraction analysis of the composites was performed using an acid digestion method as described in ASTM D3171. By this method small weighed amounts of the composites were boiled in concentrated sulphuric acid, until all the resin dissolved. The remaining glass fibres were dried and the fibre weight fraction was calculated using the known densities for the two phases and the resultant volume fractions are shown below:

Table 5

Fibre volume fractions in both the skin and core regions for all samples studied

Sample	Volume Fraction (%)
Long GL/PA MLF	29.5
Short GL/PA MLF	28.3

The volume fractions for these materials are clearly similar and within the limits expected at the weight fraction of glass fibres used.

In conclusion the analysis of the microstructures for the mouldings under consideration have revealed that certain of the terms identified in equation (1) are similar. These include E_f, V_f, E_m, FOD, γ. The fibre length distributions are clearly different so these mouldings can be taken to represent the idealised case where all the key microstructural variables are constant, with the exception of the fibre aspect ratio between the two compounds. consequently, by varying the key linear viscoelastic variables and the effect of conditioning, the influence of the fibre aspect ratio on mechanical properties for this class of material can be seen. This is explored more fully in the next section. The influence of the microstructural variables on properties is also described in section 5 where various stiffness models are presented based on the information described above.

4. MECHANICAL PROPERTY EVALUATION

The consequence of the morphological difference in terms of mean fibre aspect ratio detailed in section 3 has been examined in terms of stiffness and strength measured in both tension, flexure and torsion. Parallel sided specimens with 0° orientation with respect to the direction of applied load were machined out of the centre of each sample type. The tensile tests involved tensile dilatometry (described in more detail in references /13-15/) and creep (in tension, flexure and torsion as described in references /16-18/).

In recognizing the possible influence of moisture on these compounds, all specimens were dried in a vacuum oven at 80°C for 24 hours prior to testing. All tests were performed on dried specimens, while some tests were repeated after moisture conditioning in water at 100°C for 24 hours and 168 hours respectively according to ASTM 618, in order to see the influence of moisture on the mechanical properties studied. All measurements were made at 23°C in a temperature and humidity controlled laboratory, with some tests being repeated at higher temperature. Consequently controlled changes in both temperature and conditioning have been made with the aim of exploring the mechanical performance of these compounds across a range of service conditions.

4.1. Tensile Dilatometric Study

The results of the tensile dilatometric study are presented in two sections. The first details the changes in the elastic constants (modulus and lateral contraction ratios) and tensile strength with changes in temperature and conditioning that are representative of service conditions for this class of compound. From the reported data, the direct benefit from using an improved fibre aspect ratio on properties has been evaluated, using the methodology outlined in the Appendix. In the second section, the resultant deformation characteristics for these materials have been studied under changes of conditioning at 23°C. Evidence is presented for a change in deformation mechanism through changes in applied load and conditioning.

4.1.1. Elastic constant and tensile strength measurements using tensile dilatometry

Tensile deformation of parallel sided specimens machined from the centre of the coathanger plaque mouldings allowed the measurement of tensile modulus, tensile strength, the width and thickness lateral contraction ratios, together with the volume strain for each type of material as a function of load and temperature. The specimen geometry tested had the stress aligned parallel to the mould fill direction. Each specimen had a width of approximately 12.5 mm and a gauge length of 150 mm. The deformation was performed using a screw driven 6025 Instron at a cross head rate of 1 mm/min, with strain measurements being monitored in three mutually perpendicular directions, together with the applied stress. The temperature for testing was performed at 23°C and at 60°C. The equipment and method for calculating the volume strain are described more fully in references /14,15/. The measured values for the engineering constants of modulus (taken at 0.2% axial strain), lateral contraction ratios in the width and thickness directions (determined from the slope of the lateral/axial strain up to 0.5% axial strain) and the strength are shown in Tables 6 and 7 below:

Taking the data tested at 23°C and at 60°C, in both the dry and conditioned (168 hrs) state allows the analysis of the data contained in Tables 6 and 7 to be conducted using a 2^3 factorial experiment /19,20/, with the key variables being examined as the effect of fibre aspect ratio (Long vs Short), effect of humidity (Dry vs Wet sample state) and effect of temperature (23°C vs 60°C). The average effect across all three variables can be determined simultaneously, thus allowing for a statement to be made on the influence of fibre aspect ratio on the stiffness and strength. The methodology is explained in more detail in the Appendix and the key conclusions are repeated below.

The 2^3 factorial experiments showed that:

a) The Long GL/PA MLF mouldings show higher stiffness values compared to the equivalent Short GL/PA MLF mouldings at all temperatures and under all levels of humidity. The mean result is an increase in modulus of 1.4 GPa for pultrusion based compounds compared to the mouldings produced by extrusion based compounding across the service conditions outlined. This result is statistically significant compared to the ±95% confidence level given from a t-test based on the experimental data and represents an average benefit of a 14% improvement in stiffness. The effect is principally due to the improved mean fibre aspect ratio found in the Long GL/PA MLF mouldings compared to the short GL/PA MLF mouldings.

b) The strength data indicate the Long GL/PA MLF mouldings show higher values compared to the equivalent Short GL/PA MLF mouldings at all temperatures and under all levels of humidity. The mean result is an increase in strength of 23 MPa by using pultrusion technology compared to the mouldings produced by extrusion based compounding across the service conditions outlined. This result is statistically significant compared to the ±95% confidence level given from a t-test based on the data. This represents an average benefit of an 18% improvement in strength. This affect is also principally due to the improved mean fibre aspect ratio found in the Long GL/PA MLF mouldings compared to the Short GL/PA MLF mouldings.

c) There is a considerable influence on the stiffness and strength in varying the service conditions from 23°C and the dry state to 60°C and the moisture conditioned state. The temperature and moisture affect the compounds through the matrix by a combination of both linear viscoelasticity and plasticisation of the nylon matrix /21/. Best service performance will be found for applications based at 23°C and under dry conditions. Raising the temperature and the moisture level reduces both the stiffness and strength accordingly.

The lateral contraction ratios have not been subjected to this analysis, but a simple inspection of the values measured show that the temperature and level of conditioning dramatically increase the values of the lateral contraction ratios. This is indicative of a fundamental change in the matrix, hence compound behaviour, due to viscoelastic effects and to plasticisation of the nylon from moisture /21/. These effects will alter the deformation characteristics for the compounds with temperature and level of conditioning as revealed in the next section.

4.1.2. Deformation mechanisms studied using tensile dilatometry

The measurement of volume strain during a tensile test

Table 6

Tensile modulus, width and thickness lateral contraction ratios (all measured at 0.2% applied strain) for all sample types at a thickness of 3 mm. The tests were performed at 1 mm/min speed and at 23°C in the dry and conditioned state. The mean results from three specimens are quoted.

Material	E GPa	LCR (W)	LCR (T)	σ (MPa)	Condition
Long GL/PA MLF	15.64 11.36 8.95	0.37 0.52 0.51	0.37 0.44 0.40	195 121 115	Dry Wet 24H Wet 168H
Short GL/PA MLF	14.69 9.37 6.57	0.42 0.49 0.50	0.36 0.38 0.42	171 135 90	Dry Wet 24H Wet 168H

Table 7

Tensile modulus, width and thickness lateral contraction ratios (all measured at 0.2% applied strain) for all sample types at a thickness of 3mm. The tests were performed at 1 mm/min speed and at 60°C in the dry and conditioned state. The mean results from three specimens are quoted.

Material	E GPa	LCR (W)	LCR (T)	σ (MPa)	Condition
Long GL/PA MLF	11.79 7.57	0.49 0.43	0.39 0.39	152 87	Dry Wet 168H
Short GL/PA MLF	10.65 6.39	0.54 0.54	0.48 0.48	123 74	Dry Wet 168H

provides an insight into the various deformation mechanisms that govern material behaviour, as well as monitoring the important engineering constants such as the modulus-strain function and the lateral contraction ratios for the material /13-15/.

The volume strain can be expressed by:

$$V_S = (1+\epsilon_A)(1-\nu_W\epsilon_A)(1-\nu_T\epsilon_A)-1 \qquad (3)$$

On expansion of this equation, the volume strain V_S can be expressed as:

$$V_S = \epsilon_A(1-(\nu_W+\nu_T))+ \epsilon_A^2(\nu_W\nu_T-(\nu_W+\nu_T))+\epsilon_A^3\nu_W\nu_T \qquad (4)$$

Thus it can be seen that the volume strain, V_S, contains first, second and third order terms that are based on the axial strain and the width and thickness lateral contraction ratios ν_W and ν_T.

It is possible to monitor the mechanisms involved in bulk deformation by comparing the change in the volume strain with an increasing stress. The major contribution involves the normal, elastic response due to hydrostatic tension in the bulk of the material under stress, defined by equation (5). In addition other mechanisms will contribute to the volume strain increase as the stress is increased. The basic shape of the volume strain/axial strain plot enables the distinction between the normal state of hydrostatic deformation, and further mechanisms of cavitation or yield to be distinguished, as explained in references /14,15/. The volume increasing mechanisms include crazing, voiding, microdebonding; shear yield mechanisms include shear band formation. The region of hydrostatic deformation can be calculated for the compounds under examination by inserting the small strain (<0.2%) values for the width and thickness lateral contraction ratios as found in Tables 6 and 7 into equation (4). The onset of a volume increasing mechanism can be seen as a large departure from the predicted volume strain behaviour in the region of hydrostatic tension, under increasing strain. Figures 4 - 7 show the stress-axial strain and the volume strain-axial strain plots for all the compounds tested at 23°C. Table 8 shows the deformation mechanism observed at high strains for all the compounds.

The predicted results for the volume strain-axial strain plot for the Long GL/PA MLF in the dry and partially conditioned state are in good agreement with the measured value for the volume strains, indicating that the deformation up to 1.00% applied strain is primarily dilational in nature. For the Long GL/PA MLF compound under more extreme conditioning and for the Short GL/PA MLF compound under all levels of conditioning, the predicted result is somewhat smaller than the measured value for the volume strain. This indicates that an extra volume increasing mechanism is occurring at high levels of applied strain. The likely candidate for this mechanism is some form of interfacial failure, which might include debonding at the fibre matrix interface. This has been observed from a cursory examination of the failure surface of these compounds by SEM. For the short GL/PA MLF moulding this occurs at a stress of 115 MPa (in the dry state) and 58 MPa (in the conditioned state). For the Long GL/PA MLF compound the volume increasing mechanism occurs at 55 MPa (in the conditioned state). It is clear, however, from the tensile dilatometric study that the short GL/PA MLF compound is more susceptible to the volume increasing mechanism with applied strain and changes in conditioning than for the Long GL/PA MLF compound. The explanation for this is not immediately apparent given that the degree of adhesion between the glass fibres and the nylon matrix in the two materials is similar.

4.2. Creep Study

In this section the results of a series of tensile, flexural and torsional creep studies are reported. The tensile creep study was based on a series of specimens studied at various temperatures and conditioned in the dry state. The flexural and torsional creep data were all performed on specimens tested under dry conditions and at 23°C.

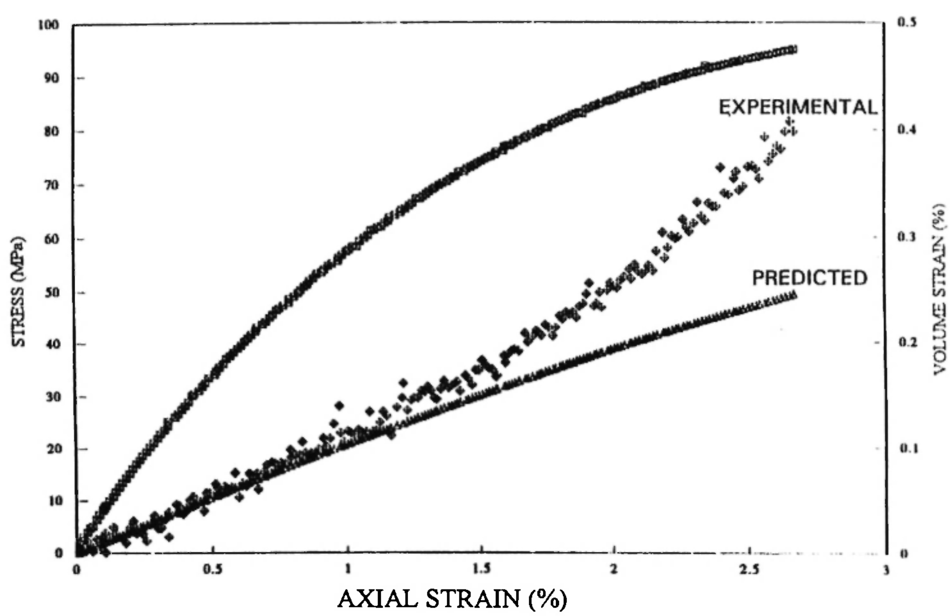

Fig. 4 Long GL/PA MLF (23°C Dry) Stress and volume strain vs axial strain

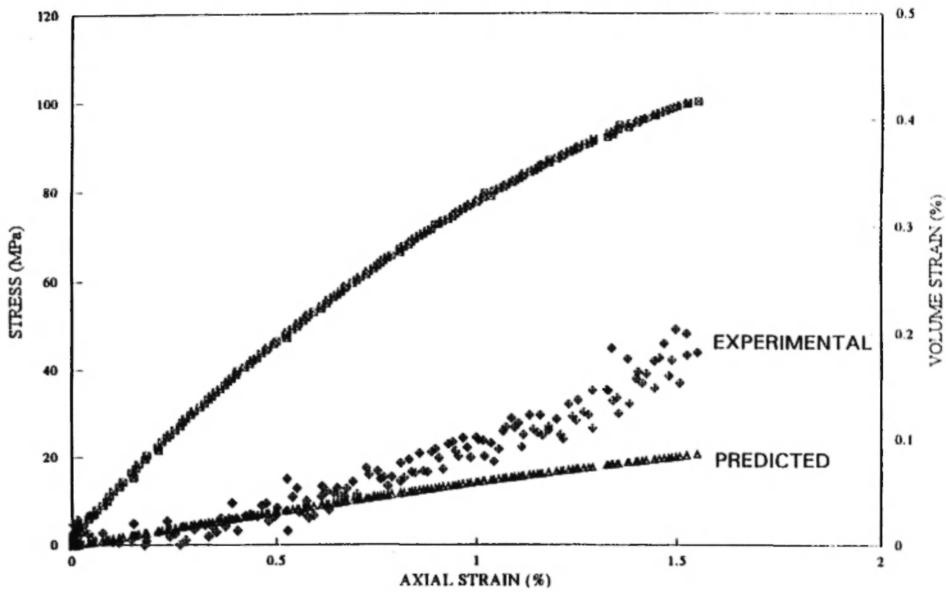

Fig. 5 Long GL/PA MLF (23°C Wet) Stress and volume strain vs axial strain

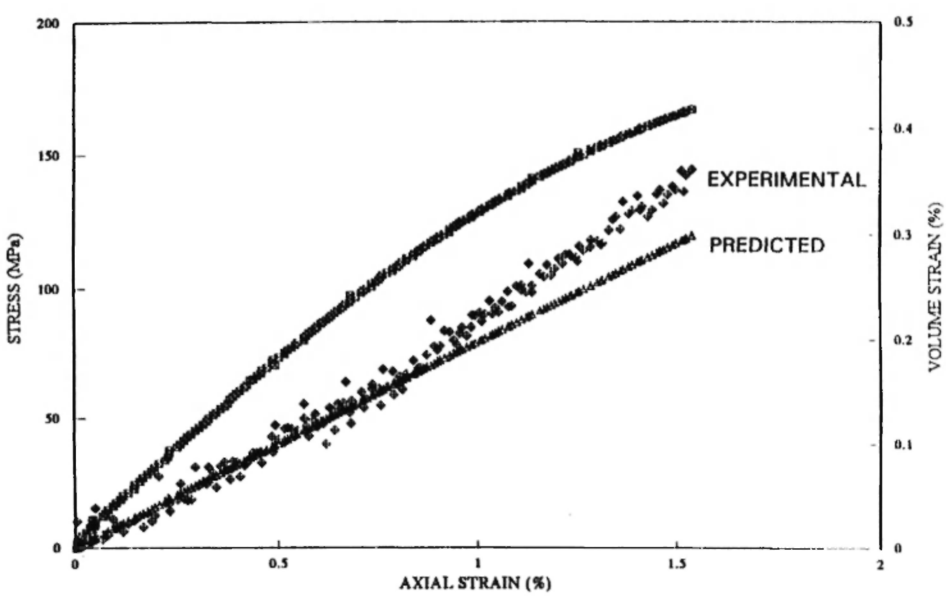

Fig. 6 Short GL/PA MLF (23°C Dry) Stress and volume strain vs axial strain

4.2.1. Tensile creep study

The 100 second isochronous tensile modulus and the resulting creep function measured at approximately 0.4% strain was determined for both the Long and Short GL/PA MLF compounds at 23°C in the dry and conditioned state (168 hours) and at 60°C and 120°C under dry conditions using the method described more fully by Turner /16/. The creep functions for the Long and Short GL/PA MLF compounds tested at 23°C, 60 °C and 120°C in the dry state are shown in Figures 8 and 9 respectively. The 100 second isochronous modulus data are shown in Table 9.

As can be seen from the data in Table 9 and from the creep functions displayed in Figures 8 and 9, the

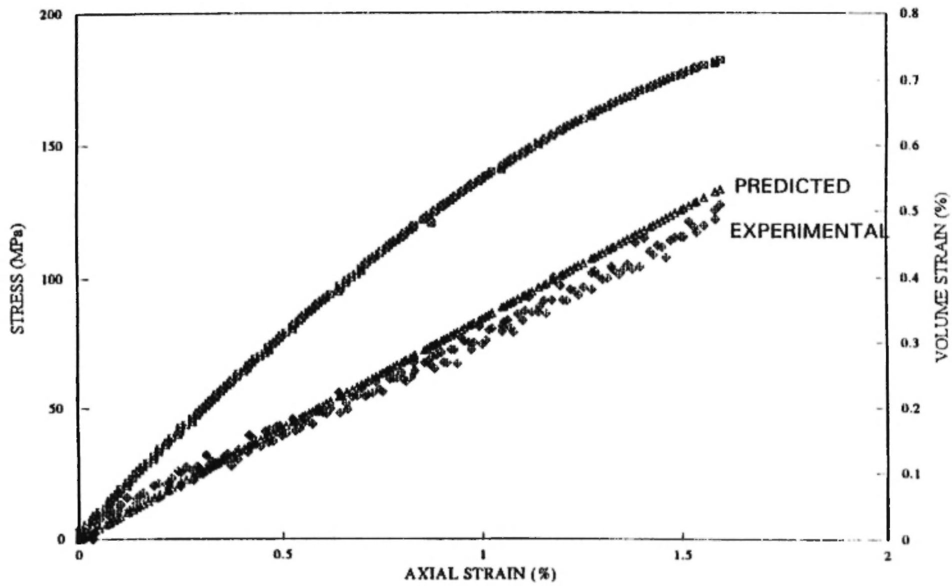

Fig. 7 Short GL/PA MLF (23°C Wet) Stress and volume strain vs axial strain

Table 8

Deformational behaviour observed from the plots of volume strain-axial strain as found from Figures 4 - 7. The predicted volume strain responses are calculated from the experimentally determined lateral contraction ratios and are plotted as lines while the experimental volume strain data are plotted as individual points.

Material	Condition	Deformation Mechanism at high strain
Long GL/PA MLF	Dry Wet 24H Wet 168H	Dilational Dilational Volume Increasing
Short GL/PA MLF	Dry Wet 24H Wet 168H	Volume Increasing Volume Increasing Volume Increasing

Table 9

100 second creep modulus data determined by interpolation at 0.2% strain at 23°C, 60°C and 120°C for both the Long and Short GL/PA MLF mouldings tested in the dry state.

Material	100s E GPa 23°C	100s E GPa 60°C	100s E GPa 120°C	Condition
Long GL/PA MLF	15.4	9.10	7.9	Dry
Short GL/PA MLF	14.9	8.46	5.4	Dry

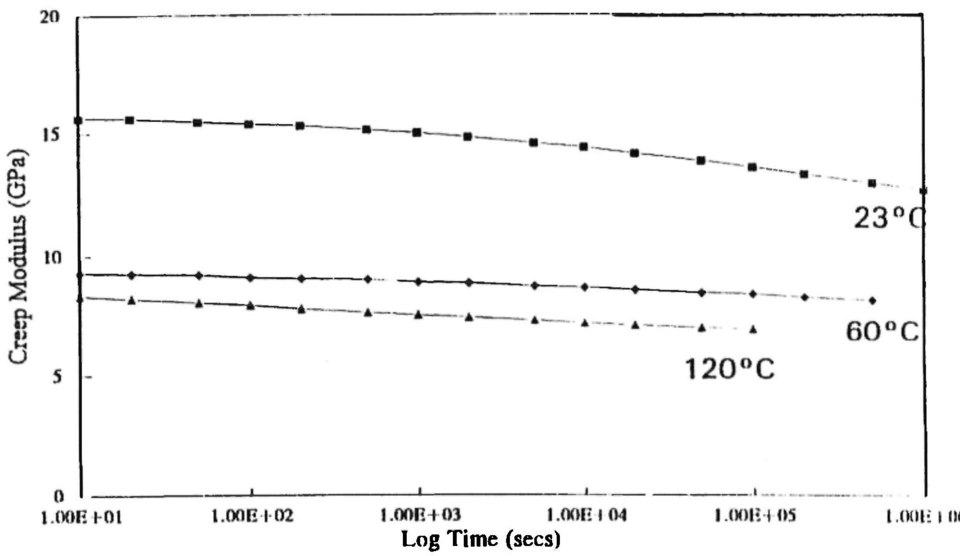

Fig. 8 Creep modulus for long GL/PA MLF mouldings

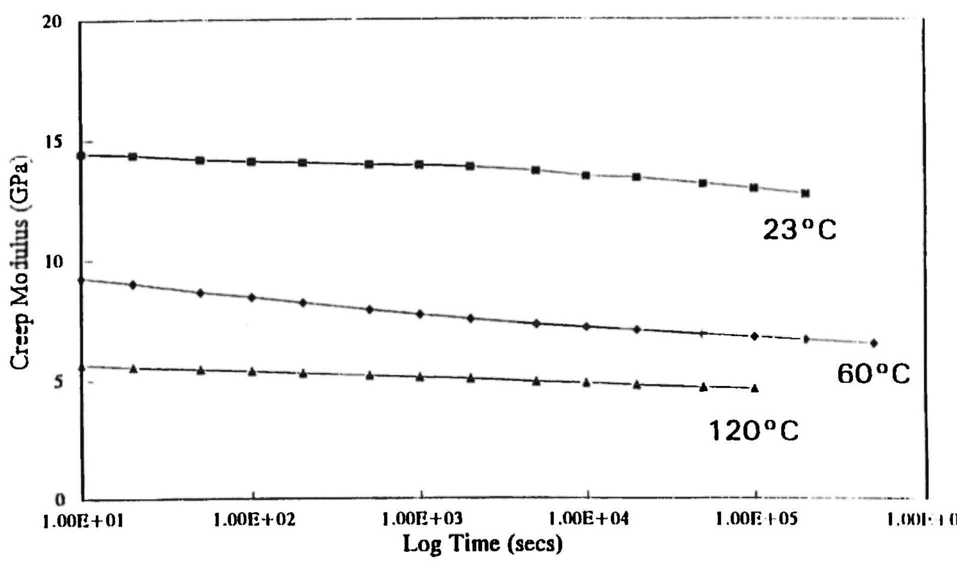

Fig. 9 Creep modulus for short GL/PA MLF mouldings

Long GL/PA MLF mouldings show improved stiffness at low strains compared to the Short GL/PA MLF mouldings at all temperatures, which is a result consistent with those reported from the tensile dilatometry study. The creep function for the Long GL/PA MLF compound showed improved performance with temperature and time compared to the equivalent creep functions for the Short GL/PA MLF compound.

The influence of moisture on creep performance can be seen in Figure 10. The 100 second and 10^5 second creep modulus data are shown in Table 10.

As can be seen from this data, the Long GL/PA MLF compound retains its creep modulus better than the short GL/PA MLF compound under the influence of both time and conditioning.

Using a 2^3 factorial experimental analysis (see

Table 10

100 second and 10^5 second creep modulus values determined by interpolation at 0.2% strain at 23°C for both the Long and Short GL/PA MLF mouldings tested in the dry and conditioned state.

Material	10^2 s E GPa 23°C	10^5 s E GPa 23°C	Condition
Long GL/PA MLF	15.4 14.2	13.6 10.8	Dry Wet 24 H
Short GL/PA MLF	14.9 11.9	12.9 8.6	Dry Wet 24 H

Table 11

100 second isochronous flexural creep modulus, determined at 0.2% strain and at 23°C.

Material	E GPa 23°C	Condition
Long GL/PA MLF	14.59	Dry
Short GL/PA MLF	14.76	Dry

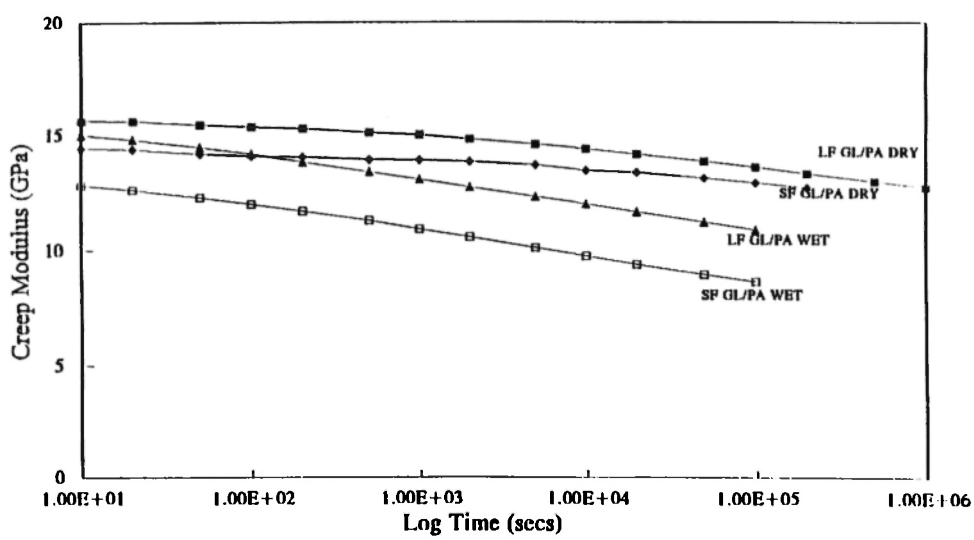

Fig. 10 Creep modulus for long and short GL/PA MFL mouldings at 23°C Influence of conditioning on creep

appendix 3) showed that the Long GL/PA MLF mouldings showed improved creep modulus values compared to the equivalent Short GL/PA MLF mouldings at all times and under all levels of humidity. The mean result is an increase in modulus of 1.4 GPa from using pultrusion based compounding compared to extrusion based technology across the service conditions outlined above. This is a similar result found for the effect of conditioning by the factorial analysis of the data by tensile dilatometry for a different set of service conditions. The influence of time under load (from 100 seconds to 10^5 seconds acts to reduce the modulus by 2.6 GPa across all compounds) and conditioning the samples reduces the modulus by 2.8 GPa. Changes in both the time and temperature regime explored will adjust the resultant modulus for these materials, but it is expected that the Long GL/PA MLF compound would outperform the Short GL/PA MLF compound under a common temperature and time under load.

4.2.2. Flexural creep study

The 100 second flexural creep modulus was determined using the method described by Turner *et al.* /18/. The data measured at 23°C in the dry state are shown below in Table 11.

These values should be compared to the isochronous creep modulus values reported in Table 9. In conventional mouldings, the flexural modulus values are generally higher than the tensile modulus values. This is due to the presence of a skin/core/skin microstructure, given that flexural loading preferentially loads the skin regions of a beam. The flexural creep modulus values are slightly smaller than the tensile values, which directly shows the influence of multilive feed processing on the material microstructure. Consequently, the equivalence of the tensile and flexural creep modulus values indicate that the multilive feed technique has removed most of the skin/core/skin microstructure confirming the observations made directly by the microstructural examination reported in section 3.

4.2.3. Torsional creep study

The 100 second torsional creep modulus was determined using the method described by Dunn and Turner /17. The data measured at 23°C in the dry state are shown below in Table 12.

The data show little difference in shear modulus determined about the 0° direction (equivalent to G_{12} in a unidirectional composite), which again reveals that both the Long and Short GL/PA MLF have a similar microstructure.

Table 12

100 second isochronous torsional creep modulus, determined at low strain and at 23°C.

Material	G GPa 23°C	Condition
Long GL/PA MLF	2.35	Dry
Short GL/PA MLF	2.27	Dry

5. MODEL FOR STIFFNESS AND STRENGTH OF DISCONTINUOUS FIBRE COMPOSITES

It is of some interest to consider from a theoretical point of view the stiffness and strength of the compounds produced by multilive feed technology. In section 5.1 the influence of fibre length, diameter and matrix modulus on the predicted composite modulus in tension are examined. In section 5.2 the influence of fibre length on the predicted strengths for the Long and Short GL/PA MLF compounds are explored.

5.1. Models for the Stiffness of Discontinuous Fibre Compounds

In order to comment on the relative moduli values for these two materials it is helpful to have some knowledge of the expected moduli values for identical microstructural arrangements for these materials. Naturally, these expected moduli values must reflect the material differences between the composites such as different fibre length distributions, different fibre diameters, etc. There are many models available for the prediction of modulus for discontinuous fibre composites. Three useful models, recently reviewed by Darlington and Christie /22/ are used for predicting the tensile stiffness of the Long and Short GL/PA MLF compounds at a range of temperatures. The Cox model /23/ can be used to predict the tensile modulus as described by Bailey *et al.* /5/ in discontinuous fibre composites. The model adopted is based on a non-interacting layer approach where each layer contains fibres with a single orientation. Two other useful models have also been used; those by Halpin-Tsai /24/ and by Ogorkiewicz and Weidmann /25/. The mathematics behind each of these models are not presented here; interested readers should consult reference /22/ for details. The three models are abbreviated using the nomenclature Cox, H-T and O-W for simplicity.

In order to use the models in real composite structures, account has to be made of the fibre lengths, orientations and volume fractions in the moulded part under consideration. This is usually an extremely complicated step to perform and involves a full microstructural characterisation as described in section 3. For the Long and Short GL/PA MLF mouldings under present consideration, a few simplifying assumptions are made before calculating the stiffness in tension. These are:

1. Only the mean fibre aspect ratio is used in the calculation.
2. The fibre orientation distribution is assumed to be represented by a single angle, Θ, which is the mean angle for the fibres in the moulding. This value of Θ is used to adjust the predicted stiffness of a unidirectional discontinuous fibre composite through the use of the multiplicative Krenchel function /26/, $\cos^4\Theta$. For these mouldings only a single layer is assumed, so the assumption of using a single Θ is valid. For the purposes of the calculations presented it is assumed that the average value of the X and Z components (measuring the degree of fibre orientation with respect to the direction of fibre flow) through the thickness of the mouldings are equivalent to the Krenchel function. This information can be calculated from the data held in Table 1.
3. The fibre volume fraction is fixed constant between both modelled compounds.

With these assumptions in place, it is possible to see the influence of the mean fibre aspect ratio on the predicted stiffness with changes in matrix modulus due linear viscoelastic effects such as temperature, time, strain, etc. /24/. Note that the models assume the compounds are in the dry state.

In order to proceed with the calculations of modulus, the parameters contained in Tables 13 and 14 were input into the model. Table 15 summarises these calculations in comparison with the measured values, as reported in Tables 6, 7 and 9.

In view of the simplicity of the models and the input data, it can be seen that the agreement between the predicted and measured moduli are good. The mean difference between the three models and the experimental data are to within ±15% at all temperatures. The Long GL/PA MLF compounds are always predicted to have the higher stiffness, as observed in all experiments. It can therefore be

Table 13

Material property input data used in the model for stiffness at low strain. Note the change in matrix modulus and lateral contraction ratio LCR with increasing temperature.

Model Input	Value 23°C	Value 60°C	Value 120°C
Ef (GPa)	76	76	76
Em (GPa)	2.8	1.5	0.5
Diameter Long GL/PA microns	17	17	17
Diameter Short GL/PA microns	10	10	10

Table 14

Microstructural property data used in the model for stiffness at low strains. The data are representative of the microstructural information found in Tables 2, 3 and 5 for the fibre orientation, mean fibre length and volume fraction respectively.

Model Input	Vf	Mean Fibre Length mm	Krenschel function
Long GL/PA MLF	0.30	0.60	0.76
Short GL/PA MLF	0.30	0.20	0.67

Table 15

Measured tensile modulus at 23°C, 60 °C and 120°C together with the calculated modulus values from the three models (Cox, H-T and O-W) described above.

Material	E GPa Measured·	E GPa Calculated Cox Model	E GPa Calculated H-T Model	E GPa Calculated O-W Model	Temp°C
Long GL/PA MLF	15.95 11.79 7.94	16.72 15.81 12.62	15.43 12.57 7.33	16.23 13.73 8.74	23 60 120
Short GL/PA MLF	14.93 10.65 5.37	13.33 11.52 7.78	12.05 9.11 4.58	12.99 10.30 5.99	23 60 120

concluded that the difference in microstructures, particularly the fibre length distributions for the two materials, is the reason for the difference in measured moduli. The model indicates that the longer fibres achieved through the use of pultrusion technology should result in stiffer compounds, compared to compounds made by extrusion compounding, with a smaller resultant fibre length distribution. Given the differences in fibre length distributions found in the compounds as described in section 3.2, it is worth considering why the stiffness for the Long GL/PA MLF moulding is not significantly greater than that for the Short GL/PA MLF compound at room temperature.

5.2. Influence of Mean Fibre Aspect Ratio on Stiffness of Discontinuous Fibre Composites

In a recent review paper the influence of fibre aspect ratio on the deformation of injection moulded discontinuous fibre reinforced composites was described in terms of the Cox model /27/. It was found that the critical fibre length for a particular fibre/resin combination varied linearly with the fibre diameter, as the root of the fibre/matrix tensile modulus and as the inverse root of the fibre volume fraction. The experimentally determined values for critical fibre length determined from single fibre tests gave values far larger than those calculated for more realistic mouldings at higher volume fractions. The values for critical fibre length for a 50% w/w glass fibre/polymer composite as determined from the Cox model paper are shown in Table 16.

Given these values for the critical fibre lengths for glass fibres with diameters at 10 and 17 microns (the diameters used for the Long and Short GL/PA MLF compounds) the percentage of fibres with lengths in excess of the critical fibre length as found from the fibre length distributions described in section 3.2 are shown in Table 17.

This implies that at room temperature (where the matrix modulus has a value of approximately 3GPa) both the Long and Short GL/PA MLF compounds have the majority of their fibres with lengths greater than the critical fibre length and so are acting as good composite materials. Consequently both types of compound would be expected to show similar deformational behaviour at low strains and times. At the higher temperature of, say 60°C, the modulus value for the nylon approximately halves (to 1.5 GPa in the model). At this new value for the matrix modulus, the critical fibre length changes accordingly. The Long GL/PA MLF compound still has the majority of its fibres greater than the critical fibre length, whereas the Short GL/PA MLF compound has approximately only two thirds of its fibres with lengths greater than the critical fibre length. On the basis of this argument it is expected that the Long GL/PA MLF compound would show an improved modulus compared to the Short GL/PA MLF compound. This is in accordance with the data found for the tensile dilatometry and tensile creep studies at elevated temperature. It is worth noting that the influence of moisture acts to reduce the modulus of nylon through plasticisation, so at room temperature tests conducted in the conditioned state might be expected to show property benefits for the Long GL/PA MLF compound compared to the Short GL/PA MLF compound. Again this is in accordance with the experimental evidence. Consequently the analysis described above indicated that a larger mean fibre aspect ratio for a discontinuous fibre compound directly improves the stiffness for this class of compound. The relative stiffness advantage found for a compound with a larger mean fibre aspect ratio will improve as service conditions due to viscoelasticity (time, temperature, strain, etc.) or due to conditioning act to soften the matrix material. A similar effect was experimentally noted in a previous study /3/ based on an evaluation of Long and Short

Table 16

Predicted critical fibre lengths for a unidirectional discontinuous glass fibre reinforced composite with Vf - 0.30, with varying fibre diameters and matrix moduli. The data for the critical fibre lengths are given in microns.

Fibre Diameter (μm)	E = 2.8 GPa	E = 1.5 GPa	E = 0.5 GPa
10	98	135	233
17	167	229	396

Table 17

% Fibres as determined from an average of 1000 fibres in the skin and core region of the Long and Short GL/PA MLF mouldings with lengths greater than the critical fibre length found from Table 16 for a particular matrix modulus and fibre diameter value.

Sample + mean fibre diameter	% Fibres with length > lc (with E = 2.8 GPa)	% Fibres with length > lc (with E = 1.5 GPa)
Long GL/PA MLF (17 μm)	98%	95%
Short GL/PA MLF (10 μm)	85%	68%

40% w/w GL/PP compounds produced by standard injection moulding, though the exact explanation for the relative performance between the two compounds was not described using the analysis presented above.

5.3. Model for the Strength of Compounds

Modelling the strength of discontinuous fibre composites presents some challenges, since the methodology is not as well advanced compared to the analysis used to predict stiffness. Account needs to be taken of the fibre length distributions and orientations within a moulding as well as the fibre volume fraction. This is similar to the considerations made for stiffness; however, the mechanisms for composite strengthening are not so well understood compared to the mechanisms for stiffening the compound. For the simplest case of unidirectional discontinuous fibre reinforcement it is thought that there are two principal mechanisms involved which relate to the fibre length distribution. For fibres less than the critical fibre length, the applied stress will probably initiate a failure involving the matrix via an interfacial shear failure (see for example Hull /28/ for a review of the theory and Galiotis /29/ and Sato /30/ for a review of the micromechanics for discontinuous fibre reinforcement and interfacial breakdown between fibre and matrix); for fibres greater in length than the critical fibre length, the failure will involve principally fibre fracture. The theory, however, assumes that only one value for fibre strength is used in predicting the eventual composite strength by this mechanism. It is well understood that the fibres in a composite will have a range of strengths, described by the Weibull distribution for the particular fibre bundle under consideration, so the strength model automatically assumes a simplification of a more complicated situation (however the assumption of a single value for fibre modulus in stiffness calculations is well accepted). The model for unidirectional discontinuous fibre strength can be given by the following expression:

$$\sigma = \Sigma\left(\frac{l_i \tau}{d}\right)V_i + \Sigma\left(1 - \frac{l_c}{2l_j}\right)\sigma_f V_j + \sigma_m(1 - V_f) \qquad (8)$$

The first term is used to sum the contribution due to the first process defined earlier (interfacial failure), whereas the second term sums the contribution due to the second mechanism described, that due to fibre failure. It was noted in section 5.2 that the majority of fibres in the fibre length distribution for both the Long and Short GL/PA MLF compounds were greater than the critical fibre length at room temperature, so the major contribution to the compound strength will come from the second mechanism. It is interesting o note from equation (8) that the fibre diameter, hence fibre aspect ratio, only influences the first term in the expression. Consequently, for an imaginary experiment for two compounds with equivalent mean fibre lengths longer than the critical fibre length but different fibre diameters, equation (8) would predict the same strength for the two compounds. Models for the stiffness of the same two compounds would predict a stiffer material for the compound with the smaller fibre diameter.

Given that a range of fibre orientations is normally present in a discontinuous fibre composite, the strengths given by equation (8) need to be multiplied by a factor that accounts for the FOD. This is usually a term similar in nature to the Krenchel factor.

Another method that takes into account the uncertainties of describing the strength of these compounds is to model the strength as being composed of three layers, one from the model outlined in equation (8) and two layers with strengths given by that due just to the matrix, corrected for the volume fraction content. This method weights the matrix contribution more heavily than assumed by equation (8).

The two models outlined above have used the following parameters as input values.

Fibre strength	=	1800 MPa
Matrix strength	=	70 MPa (23°C)
	=	40 MPa (60°C)
Vf	=	0.30
d	=	17, 10μm (for the two compounds)

and the FLD for the Long and short GL/PA MLF mouldings as given by Figure 4.

The results from the two models are given below:

The prediction made by the full composite strength model (equation (8) – data given as Model (1) in Table 18) gives an overestimate of the composite strengths of

Table 18

Predicted strengths for Long and Short GL/PA MLF via Model (1) (via equation (8) weighted with matrix contribution) as described above compared to the experimental data measured at 23°C and 60°C in the dry state.

Sample	T = 23°C			T = 60°C		
	Model 1	Model 2	Exp.	Model 1	Model 2	Exp.
Long GL/PA MLF	506	215	195	451	177	152
Short GL/PA MLF	438	179	171	374	143	123

some 2.6 for both the Long and Short GL/PA MLF compounds at 23°C and by a factor of 3 at 60°C. The Krenchel factor will reduce these values using a term related to the mean fibre orientation, $\cos^4\Theta$, although the values suggested for stiffness modelling would not be sufficient to account for the discrepancy between the model and experiment.

The predictions made by the second model are within 10% of experiment. Consequently, although Model 2 has less justification in terms of rigorous theory, it is a better guide to the prediction of strengths in these types of materials than Model 1.

Both models predict that the Long GL/PA MLF compounds have a larger strength than the short GL/PA MLF compound, as seen in experiment. This is a direct consequence of having a longer mean fibre length and represents a real property benefit. Reference /27/ described at the micromechanical level how the fibre aspect ratio directly relates to an improvement in stiffness in this class of material across a range of service conditions. The appropriate guideline for improved performance could be defined to aim for a mean fibre aspect ratio which is four times greater than the critical fibre aspect ratio across the range of service conditions anticipated. Under current technology pultrusion based compounding offers the best available route for achieving this aim.

6. CONCLUSIONS

This paper has explored the influence of the fibre fibre aspect ratio on stiffness and strength in a series of multi-live feed injection mouldings, based on 50% w/w GL/PA made from pultrusion and extrusion based compounding. The microstructural characterisation of these mouldings revealed that certain key variables such as fibre orientation, volume fraction and adhesion were found to be similar between the two compounds designated Long and Short GL/PA MLF. However, the fibre length distribution, hence fibre aspect ratios between the two classes of compound, were found to be different, with the long fibre compound found to have a larger mean fibre aspect ratio compared to the extrusion based compound as found from past studies. Consequently, this study represents an opportunity to examine the role of the fibre aspect ratio on mechanical performance, with the possible complication of other microstructural variables held constant.

The mechanical property characterisation examined the stiffness and strength as a function of key viscoelastic variables, such as temperature, time and strain, by a number of test methods including tensile dilatometry and creep. The study revealed that an improved fibre aspect ratio directly benefited both the stiffness and strength, across a wide range of service conditions including conditioning, temperature, time and strain. In addition, a key change in deformational behaviour was seen, with the Short GL/PA MLF compound displaying fibre debonding at all service conditions. The Long GL/PA MLF compounds were found to display only dilation as the principal deformation mechanism at all but the most extreme service conditions, which represents another benefit in mechanical performance directly related to improved fibre aspect ratio.

The available stiffness and strength models also indicate that an improved fibre aspect ratio benefits mechanical performance, with the models correctly ranking the property performance of the two types of compound. Generally the stiffness models could predict the modulus to within 10% over a range of temperatures; the strength model provided overestimates by a large factor.

In conclusion it has been demonstrated from both experimental and theoretical grounds that an improved fibre aspect ratio in this class of compound will result in an improved mechanical property performance in terms of stiffness and strength across a wide range of service conditions.

7. ACKNOWLEDGEMENTS

The authors would like to thank Professor M. Bevis and Dr. P. Allan for processing the materials using the multilive feed process and I.D. Newton at ICI Wilton for characterising the fibre volume fraction.

8. REFERENCES

1. R.C. Stephenson, S. Turner and M. Whale, *Poly. Eng. Sci.*, **19**(3), 173 (1979).
2. P.S. Allan and M.J. Bevis, *Plast. Rubb. Proc. Appl.*, 7, 3 (1987).
3. C.R. Gore, G. Cuff and D.A. Cianelli, *Mat. Eng.*, **103** (3), 47 (1986).
4. D.R. Moore, I.M. Robinson and B. Slater, "Engineering properties of long and short glass fibre reinforced polypropylene compounds", in: "FRC 90", Inst. Mech. Eng., London, p. 203, 1990.
5. M. Davies, R.S. Bailey and D.R. Moore, *Composites*, **20** (5), 453 (1989).
6. R.S. Bailey and H. Kraft, *Int. Poly. Proc.*, **2**, 94 (1987).
7. G. von Bradsky, "Image analysis facilities at Wilton", ICI Report IC 12263.
8. G. von Bradsky and R.S. Bailey, "Measuring spatial orientation by image analysis", ICI Report IC 13808.
9. G. Fischer and P. Eyerer, *Polymer Composites*, 9, 4 (1988).
10. S. Nolan, "Fibre morphology in long fibre reinforced thermoplastics: The effect of different injection moulding techniques", Verton Background Science Report, 1990.
11. M.J. Folkes, "Short Fibre Reinforced Thermoplastics", Research Studies Press, 1982.
12. P. Hine, "Examination of ultrasonic elastic constants, morphology, and composite properties for glass fibre/nylon compounds", Private report from University of Leeds.
13. D.C. Leach and D.R. Moore, *Composites*, **16**, 113 (1985).
14. S.I. Naqui and I.M. Robinson, *J. Mat. Sci.*, **28**, 1421 (1993).
15. R.S. Bailey, D.R. Moore, I.M. Robinson and P.M. Rutter, *Sci. Eng. Comp. Mat.*, **2**, 171 (1993).
16. S. Turner, *British Plastics*, June, 1964.
17. M.J. Bonnin, C.M.R. Dunn and S. Turner, *Plast. Poly.*, p. 517, December (1969).
18. C.M.R. Dunn and S. Turner, *Plast. Poly.*, p. 26, February, 1972.
19. ASTM E1169 - 89.
20. O.L. Davies, "Design and Analysis of Industrial Experiments", Longmans, 1978.
21. T.S. Ellis, *J. Appl. Poly. Sci.*, **36**, 451 (1988).
22. M.W. Darlington and M.A. Christie, "Time dependent properties of injection moulded composites", in: The Role of the Polymeric Matrix in the Processing and Structural Properties of Composite Materials, ed. J.C. Seferis and L. Nicolais, Plenum Press, N.Y., U.S.A., 1983.
23. H.L. Cox, *Brit. J. Appl. Phys.*, **3**, 72 (1952).
24. J.C. Halpin and J.L. Kardos, *Poly. Eng. Sci.*, **16**, 344 (1976).
25. R.M. Ogorkiewicz and G.W. Weidmann, *J. Mech. Eng. Sci.*, **16**, 10 (1974).
26. H. Krenchel, "Fibre Reinforcement", Akademisk Forlag, Copenhagen, Denmark, 1964.
27. I.M. Robinson and J.M. Robinson, "A review of the influence of fibre aspect ratio on the deformation and failure of discontinuous fibre reinforced composites", ICI Report IC 14688.
28. D. Hull, "An introduction to composite materials", Cambridge Solid State Science Series,

Cambridge University Press, 1981.
29. N. Melanitis and C. Galiotis, *Proc. R. Soc. Lond. A*, 440, 379 (1993).
30. N. Sato, T. Kurauchi, S. Sato and O. Kamigaito, *J. Comp. Mat.*, **22**, 850 (1988).

APPENDIX

Factorial design of experiments based on Plackett Burmann designs

The following brief review outlines a method for examining the influence of three variables (which are thought to be independent from each other) upon a measurable quantity, whilst simultaneously describing their interactions with each other. The method is described more fully by Davies (1978) /20/ and in ASTM E1169 /19/. The method calls for a matrix designed experiment where the three declared variables are raised between a high value (+) to a low value (–) in a controlled manner using the design shown below:

Table 1

Design matrix for a Plackett-Burmann 2^3 factorial experiment

The net effect of variables A, B, C can be determined from the mean response for all the + results less the mean response of all the minuses, i.e.,

Effect A = (X2+X4+X6+X8)/4 - (X1+X3+X5+X7)/4
Effect B = (X1+X2+X5+X6)/4 - (X3+X4+X7+X8)/4
Effect C = (X1+X2+X3+X4)/4 - (X5+X6+X7+X8)/4

The interactions between each of these variables AB, BC, AC, ABC can also be determined from the mean response for all the + results less the mean response of all the minuses using the following arrangements, i.e.,

Interaction AB = (X1+X4+X5+X8)/4 - (X2+X3+X6+X7)/4
Interaction AC = (X1+X3+X6+X8)/4 - (X2+X4+X5+X7)/4
Interaction BC = (X1+X2+X7+X8)/4 - (X3+X4+X5+X6)/4
Interaction ABC = (X2+X3+X5+X8)/4 - (X1+X4+X6+X7)/4

The significance of the result of each variable and interaction can be tested using a t-test obtained using the following expression:

$$\frac{2tSD}{\sqrt{n}}$$

where t is the t-test value taken from a standard table (with ±95% confidence routinely used),
SD is the standard deviation for the experiments used,
n are the number of test results involved (8 in this instance).

Thus by t-testing the resultant effects and interactions against the ±95% confidence value, truly significant effects and interactions can be identified and other less important effects and interactions can be ignored. Thus the three variables and their possible coupling may be determined separately in an experiment that allows for the variation of each.

In the present study the three key variables are:

Variable A:
Fibre length distribution and type of fibre technology
The high term (+) are Long GL/PA MLF compounds.
The low term (–) are Short GL/PA MLF compounds.

Variable B:
Temperature in °C.
The high term (+) are tests conducted at 23°C.
The low term (–) are tests conducted at 60°C.

Variable C:
Level of moisture conditioning.
The high term (+) are tests conducted with specimens in the dry state.
The low term (–) are tests conducted with specimens being conditioned in water for 168 hours.

The two results being measured are the tensile modulus and strength, so the direct influence of the fibre length distribution, temperature and conditioning and their possible interaction through other effects on these measurable properties can be directly determined if the following experimental design is used:

Table 2

Design matrix for a Plackett Burmann 2^3 factorial experiment for Long and Short GL/PA MLF mouldings examined for stiffness and strength with variations in temperature and conditioning.

The data are taken from Tables 6 and 7 and the results for these analyses are shown in Appendices 1 and 2 for the tensile modulus and strength respectively.

The key effects on the modulus are (given in terms of significance):

1. Temperature (i.e. raising the temperature from 23°C to 60°C suppresses the modulus in both types of compounds by 5.8 GPa. This is a linear viscoelastic effect on the matrix).
2. Conditioning (i.e. changing the conditioning from the dry to wet conditioned state suppresses the modulus in both types of compounds by 2.4 GPa. This is due to plasticisation of the matrix).
3. Temperature and Conditioning (i.e. changing both these variables from the high to the low state suppresses the modulus by 1.6 GPa in both types of compound. This will be a combination of both linear viscoelasticity and plasticisation of the matrix).
4. Effect of Technology (i.e. changing from Long GL.PA MLF to Short GL/PA MLF compounds suppresses the modulus by 1.4 GPa across variations in service conditions of temperature and moisture. This is due to the improved fibre aspect ratio found in long fibre compounds compared to short fibre compounds and represents an average benefit of some 14% on the stiffness based on using long fibre technology under the range of service conditions examined).

The key effects on the strength are (given in terms of significance):

1. Conditioning (i.e. changing the conditioning from the dry to wet conditioned state suppresses the strength in both types of compounds by 69 MPa. This is due to plasticisation of the matrix and possibly to debonding effects between the fibres and matrix).
2. Temperature (i.e. raising the temperature from 23° to 60°C suppresses the strength in both types of compounds by 34 MPa. This is due to a linear viscoelastic effect on the matrix and possibly to debonding effects between the fibres and matrix).
3. Effect of Technology (i.e. changing from Long GL/PA MLF to Short GL/PA MLF compounds suppresses the strength by 23 MPa across variations in service conditions of temperature and moisture. This is due to the improved fibre aspect ratio found in long fibre compounds compared to short fibre compounds and represents an average benefit of some 18% on the strength based on using long fibre technology under the range of service conditions examined).

All the other possible interactions have been found to be statistically insignificant using this design of experiment. Consequently the benefits of using long fibre technology compared to short fibre technology as determined from the mouldings and service conditions under present considerations are an improved stiffness (by 14% on average) and strength (by 18% on average). Best service performance will be found for applications based at 23°C and under dry conditions. Raising the temperature and the moisture level will reduce both the stiffness and strength accordingly.

In Appendix 3 another experiment is presented examining the influence of time, conditioning and fibre technology on the creep modulus. The analysis is presented in the text in section 4.1.

APPENDIX 1

LF/GL PA and SF/GL PA Comparison with Temperature and Conditioning

Full (2)^3 Factorial Designed Experiment 15/04/93 *

Technology	Temp °C	Condition	Stifness GPa	(SD)	No. Data
SF	60	Wet (168H)	6.39	0.50	3
LF	60	Wet (168H)	7.57	0.50	3
SF	23	Wet (168H)	10.65	0.50	3
LF	23	Wet (168H)	11.79	0.50	3
SF	60	Dry	6.57	0.50	3
LF	60	Dry	8.95	0.50	3
SF	23	Dry	14.69	0.50	3
LF	23	Dry	15.64	0.50	3

Interactions for Independent Variables

Name	Technoiogy	Temp °C	Condition
Sign +/-	A	B	C
+	LF	23	Dry
-	SF	60	Wet (168 H)

Effect of A:-	1.4	Technology
Effect of B:-	5.8	Temp °C
Effect of C:-	2.4	Condition
Interaction AB:-	-0.4	Technoiogy Temp °C
Interaction BC:-	1.6	Temp °C Condition
Interaction AC:-	0.3	Condition Technology
Interaction ABC:-	-0.3	

Mean Result:-	10.28
SD:-	0.50

T Value:-	2.26
n:-	8.00
SD:-	0.50
+/- 95% Conf. Int:-	0.80

APPENDIX 2

LF/GL PA and SF/GL PA Comparison with Temperature and Conditioning

```
Full (2)^3 Factorial Designed Experiment                         15/04/93 *
******** ******** ******** ******** ******** ******** *
TechnologyTemp °C  Condition  Strength MPa (SD)        No. Data  *
******** ******** ******** ******** ******** ******** *
SF              60 Wet (168H)     74.00      10.00            3 *
LF              60 Wet (168H)     87.00      10.00            3 *
SF              23 Wet (168H)     90.00      10.00            3 *
LF              23 Wet (168H)    115.00      10.00            3 *
SF              60 Dry           123.00      10.00            3 *
LF              60 Dry           152.00      10.00            3 *
SF              23 Dry           171.00      10.00            3 *
LF              23 Dry           195.00      10.00            3 *
******** ******** ******** ******** ******** ******** *
Interactions for Independent Variables
******** ******** ******** ******** ******** *
Name       TechnologyTemp °C  Condition                 *
Sign +/-      A          B       C                      *
******** ******** ******** ******** ******** *
 +         LF                 23 Dry                    *
 -         SF                 60 Wet (168 H)            *
******** ******** ******** ******** ******** *
Effect of A:-              22.8 Technology              *
Effect of B:-              33.8 Temp °C                 *
Effect of C:-              68.8 Condition               *
Interaction AB:-            1.8 TechnologyTemp °C       *
Interaction BC:-           11.8 Temp °C   Condition     *
Interaction AC:-            3.8 Condition  Technology*
Interaction ABC:-          -4.3                         *
******** ******** ******** ******** ******** *
                                                        *
Mean Result:-           125.88                          *
SD:-                     10.00                          *
                                                        *
******** ******** ******** ******** ******** *
                                                        *
T Value:-                 2.26                          *
n:-                       8.00                          *
SD:-                     10.00                          *
                                                        *
+/- 95% Conf. Int:-      15.98                          *
                                                        *
******** ******** ******** ******** ******** *
```

APPENDIX 3

LF/GL PA and SF/GL PA Comparison with Time and Conditioning

Full (2)^3 Factorial Designed Experiment   16/04/93

Technology	Time s	Condition	Modulus G	(SD)	No. Data
SF	100000	WET 168H	8.60	0.50	1
LF	100000	WET 168H	10.80	0.50	1
SF	100	WET 168H	11.90	0.50	1
LF	100	WET 168H	14.20	0.50	1
SF	100000	DRY	12.90	0.50	1
LF	100000	DRY	13.60	0.50	1
SF	100	DRY	14.90	0.50	1
LF	100	DRY	15.40	0.50	1

Interactions for Independent Variables

Name	Technoiogy	Time s	Condition
Sign +/-	A	B	C
+	LF	100	DRY
-	SF	100000	WET 168H

Effect of A:-	1.4	Technology
Effect of B:-	2.6	Time s
Effect of C:-	2.8	Condition
Interaction AB:-	-0.0	TechnoiogyTime s
Interaction BC:-	-0.7	Time s Condition
Interaction AC:-	-0.8	Condition Technology
Interaction ABC:-	-0.1	

Mean Result:-	12.79
SD:-	0.50

T Value:-	2.26
n:-	8.00
SD:-	0.50
+/- 95% Conf. Int:-	0.80